ACS OMEGA

http://pubs.acs.org/journal/acsodf

Article

Preparation and Characterization of Pendimethalin Microcapsules Based on Microfluidic Technology

Yu Qin, Xinyu Lu, Han Que, Dandan Wang, Tao He, Dingxiang Liang, Xu Liu, Jiajia Chen, Chenrong Ding, Pengcheng Xiu, Chaozhong Xu, and Xiaoli Gu*

Cite This: *ACS Omega* 2021, 6, 34160−34172

Read Online

ACCESS | Metrics & More | Article Recommendations

ABSTRACT: Microencapsulation of pesticides is a promising attempt to reduce environmental pollution and prevent the active ingredients from the interference of external factors. In this paper, pendimethalin microcapsules were prepared by the interfacial polymerization of 4,4-methylenediphenyl diisocyanate (MDI) and ethylenediamine (EDA) based on microfluidic technology. Effects of the microchannel structure, reaction temperature, surfactant type, and fluid flow rates were investigated and evaluated. The results showed that pendimethalin microcapsules prepared under suitable conditions had a smooth surface, good monodispersity, a high encapsulation efficiency (96.7%), and excellent thermal stability. The size and morphology control of microcapsules were realized by adjusting the flow rates of the continuous phase and the hydrophilic monomer EDA aqueous solution. The release of pendimethalin had a sustained release characteristic that was closely related to the morphology of microcapsules. Compared with the pendimethalin emulsifiable concentrate, pendimethalin microcapsules exhibited outstanding herbicidal activity in the weed control experiments. Therefore, pendimethalin microcapsules with tunable properties were successfully obtained from the microfluidic device and showed great potential in agricultural applications.

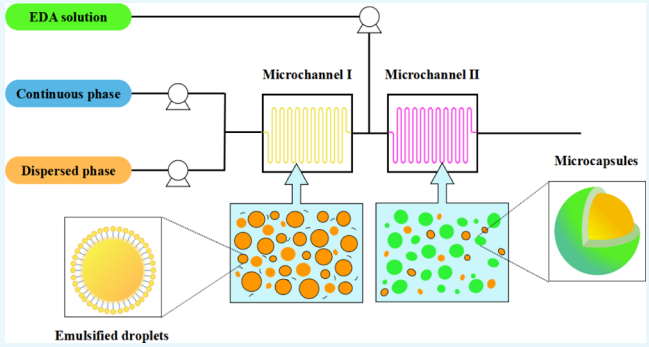

1. INTRODUCTION

With the increasing global population and food demand, pesticides are playing an increasingly important role in modern agricultural production. Pesticides can not only protect crops from pests and diseases but also improve the quantity and quality of products.[1] However, more than 90% of the applied pesticides are lost instead of acting on the targets due to their instability caused by volatilization, leaching, and degradation (photolytic, pyrolytic, and microbial).[2−5] This ineffective utilization gives rise to repeated spraying of pesticides at a high concentration, which increases the economic costs and safety hazards.[6] What is worse, excessive pesticides would cause latent environmental pollution of the soil, groundwater, and atmosphere, posing a serious threat to the ecosystem and biodiversity.[7−11] The encapsulation of pesticides has been demonstrated to be a promising remedial technique for resolving such problems to a great extent. Microcapsules refer to tiny containers with a core−shell structure, in which the core moiety is encased in the shell made of natural or synthetic polymer materials. The polymer shell can protect a susceptible active ingredient from surrounding influences and slowly release it into the environment over a specified period of time.

Some of the most commonly reported encapsulation technologies include in situ polymerization,[12,13] interfacial polymerization,[14,15] solvent evaporation,[16] suspension cross-linking,[17] and complex coacervation.[18−20] Among the above methods, the interfacial polymerization, which is the reaction of two multifunctional monomers to form a compact polymer membrane at the interface of continuous and dispersed phases, has found extensive applications in the preparation of many pesticide microcapsules for its high reaction speed, mild reaction conditions, and low manufacturing cost.[21,22] Presently, a variety of synthetic polymers have been selected as shell materials for the preparation of pesticide microcapsules, such as polyurea, polystyrene, and polymethyl methacrylate.[23] Polyurea has attracted widespread attention due to its excellent chemical resistance and mechanical and thermal properties. However, the equipment used in its industrial production is

Received: October 21, 2021
Accepted: November 26, 2021
Published: December 5, 2021

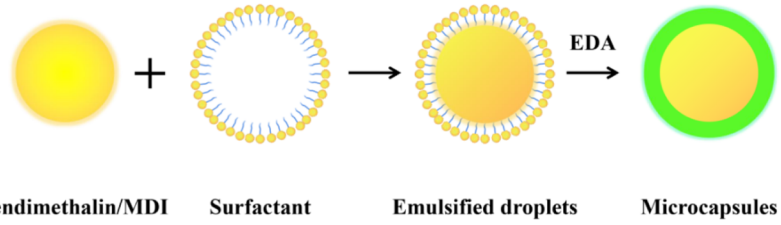

Figure 1. Formation mechanism of pendimethalin microcapsules.

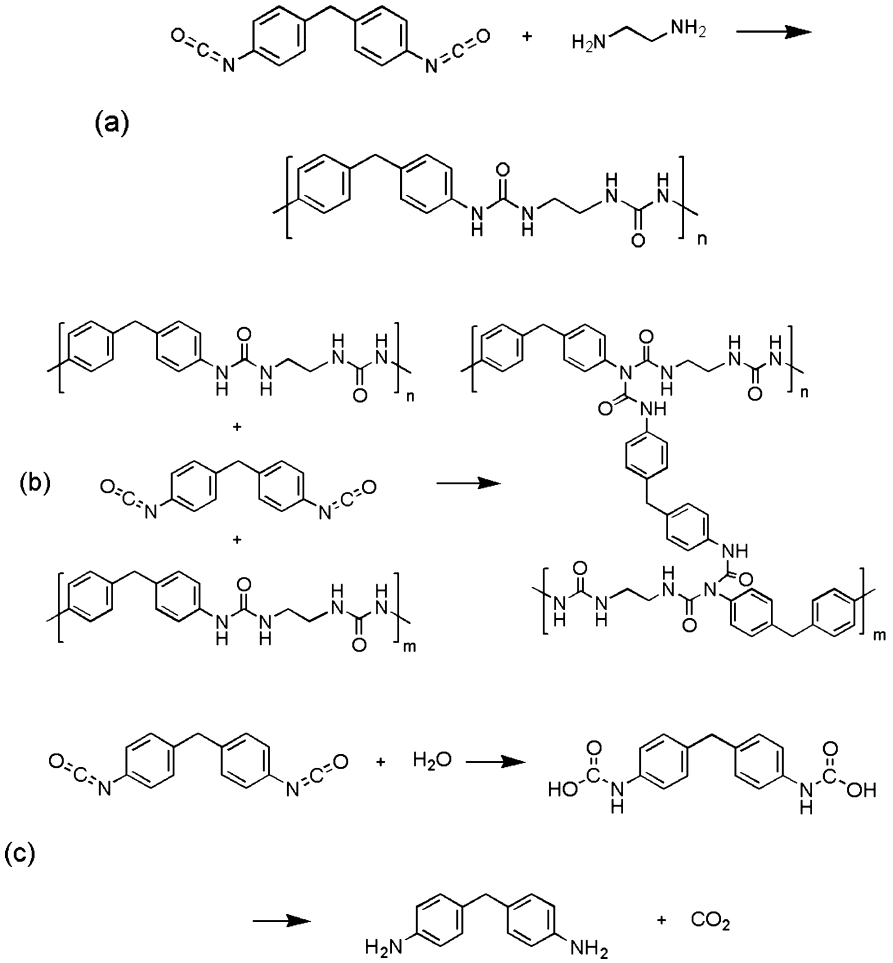

Figure 2. Possible reaction mechanism for the formation of the polyurea shell: (a) reaction of MDI with EDA, (b) cross-linking reaction between polyurea molecules, and (c) reaction of MDI with water.

usually a mechanically agitated intermittent reactor, which has certain limitations. Because of the amplification effect and nonuniform reaction, the size of particles is difficult to adjust and is widely distributed, leading to poor repeatability of the preparation, low stability of the product, and low controllability of the release behavior.[6]

The microfluidic technology is an emerging technology for generating diverse particles with well-defined structures and narrow size distributions as it affords precise flow control, as well as the ability to process trace amounts of liquid.[24,25] This method utilizes the shearing force of a flowing liquid to break up another flowing immiscible liquid into tiny droplets, which are subsequently solidified to form particles in the microchannels.[26] In recent years, the microfluidic technology has already shown superior capabilities in the manufacture of droplets, microspheres, microcapsules, and multiple emulsions with potential applications.[27−32] In the field of agriculture, microfluidic technology has been applied in the rapid trace detection of residual pesticide.[33−35] However, the fabrication of pesticide microcapsules based on microfluidic technology has been relatively rare. Zhong et al. developed a liquid-driven coaxial flow focusing (LDCFF) process for the preparation of pyraclostrobin-loaded poly(lactic-*co*-glycolic acid) (PLGA) microcapsules.[24] The microcapsule preparation based on a microfluidic device offers many advantages such as easy scalability, convenient cleaning, high reaction flux, large specific surface area, and rapid heat and mass transfer rates.[36] Besides, the process parameters can be finely adjusted to realize control over the size, porosity, surface morphology, and shell thickness of microcapsules and to further achieve the aim of a controlled and sustained release.[26]

https://doi.org/10.1021/acsomega.1c05903
ACS Omega 2021, 6, 34160−34172

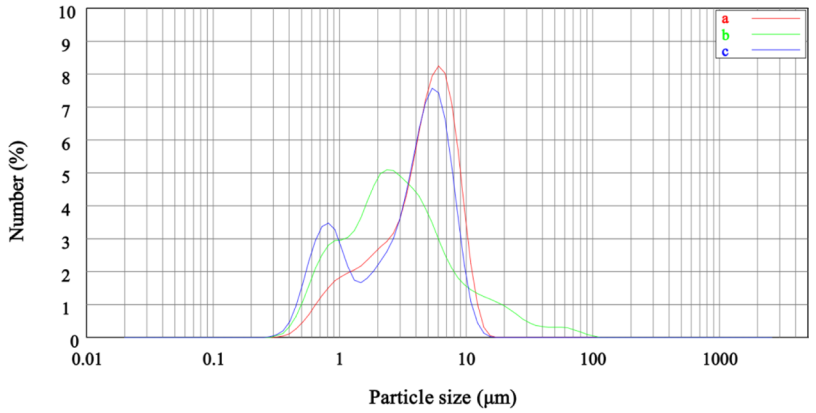

Figure 3. Particle size distribution of microcapsules prepared by microchannels with different structures: (a) heart-shaped, (b) Y-shaped, and (c) T-shaped.

Pendimethalin, a typical dinitroaniline herbicide, is mainly used for the preemergence control of most grass weeds and many broad-leaf weeds in several crops such as corn, cotton, tomato, and wheat.[37] The application of pendimethalin in the fields of agriculture is seriously restricted since it is easily lost through volatilization and photolysis.[12,37] However, the main formulation of pendimethalin is still the traditional emulsifiable concentrate (EC) owing to its poor water solubility,[38,39] which contains a large amount of organic solvents, generating unpleasant odors and resulting in great harm to humans in the spraying process.[6,38] Moreover, pendimethalin itself is highly toxic to aquatic organisms, especially to fish, requiring special attention when used in high-groundwater-level areas.[37,40] Therefore, it is of great necessity and importance to design a controlled release formulation to prevent the side effects and enhance the stability of pendimethalin.

In the past few years, a number of reports about pendimethalin encapsulation have become available,[38−42] but the work on the fabrication of microcapsules related to precise release control by using microfluidic technology has not been done. In this paper, a practical approach was proposed to prepare pendimethalin microcapsules in a simple microfluidic device. Microcapsules with pendimethalin as the core material and 4,4-methylenediphenyl diisocyanate (MDI) and ethylenediamine (EDA) as the shell materials were successfully fabricated. The effects of process parameters on the surface morphology, size, encapsulation efficiency, and thermal stability were systematically investigated. The controlled release behavior and herbicidal activity of the microcapsules were further explored. This article would provide valuable information for the industrial fabrication of pendimethalin microcapsules and reliable reference for the encapsulation of other pesticides based on the microfluidic technology.

2. RESULTS AND DISCUSSION

2.1. Preparation of Pendimethalin Microcapsules. The formation mechanism of pendimethalin microcapsules is shown in Figure 1. As the dispersed-phase fluid came into contact with the continuous-phase fluid in microchannel I, the dispersed phase rapidly broke up into tiny droplets under the influence of shearing and squeezing force.[31] Simultaneously, the stable emulsified droplets composed of pendimethalin and MDI in the continuous phase were obtained under the emulsification of the surfactant. Once in microchannel II, the MDI within the droplets and the EDA in the aqueous solution carried out interfacial polymerization at the droplet interfaces, forming solid and uniform polyurea shells surrounding the pendimethalin cores.

The possible reaction equations involved in the formation of polyurea shell are shown in Figure 2. The main scheme for the synthesis of polyurea was based on the addition reaction of the isocyanate group (−N═C═O) in MDI and amino group ($-NH_2$) in EDA (Figure 2a).[43] To be specific, when the oil-in-water (O/W) emulsion and the EDA aqueous solution were brought into contact, the MDI monomers from the dispersed phase diffused toward the oil−water interface and reacted with the EDA monomers to form polyurea in a very short time.[44] The generated polyurea precipitated at the surface and gradually formed a spherical film encapsulating the droplet.[43] As the polymerization progressed, the length of the molecule chain increased, and more polyurea was accumulated, which increased the thickness of the film layer to eventually become the complete polyurea shell. In addition, a cross-linking reaction between polyurea molecules could take place at the same time (Figure 2b), which made the polyurea shell more compact and integrated. The polyurea formation could also be accomplished through the reaction of MDI with water. Under this circumstance, the isocyanate group in MDI first reacted with H_2O to form the unstable carbamic acid (−NHCOOH), which rapidly decomposed into the amino group and CO_2 (Figure 2c).[45] The produced amino group could further react with the isocyanate group, followed by the same polymerization process described above.

The chemical structure of polyurea formed by the reaction of MDI with water was distinctly different from that formed by the reaction of MDI with EDA (Figure 2a,c). The latter is more flexible than the former due to the presence of ethylene, which was favorable for the formation of a spherical microcapsule shell.[45,46] Furthermore, the conversion of isocyanate to amine was accompanied by the release of CO_2, which existed as bubbles and may make more small pores appear on the surface of the polyurea shell.[45] Although both EDA and water could react with MDI, the reactivity of MDI toward EDA was much higher than that of water.[45,46] Hence, the reaction of MDI with EDA dominated in the formation of the polyurea shell, and the reaction of MDI with water only occurred in large quantities in the absence of EDA.

2.1.1. Effects of the Microchannel. The previous studies showed that the structure of the microchannel had a notable impact on the flow statuses of the two phases, as well as the

https://doi.org/10.1021/acsomega.1c05903
ACS Omega 2021, 6, 34160−34172

formation of emulsified droplets.[47] The particle size distributions of the pendimethalin microcapsules prepared in the different microchannels are shown in Figure 3. It can be clearly observed from Figure 3a that the distribution of microcapsules prepared by the heart-shaped microchannel presented a normal distribution, and the particle sizes were in the range of 0.71−11.14 μm with a mean diameter of about 9.62 μm. When the Y-shaped microchannel was used, the particle sizes were in the range of 0.53−10.08 μm, and the mean diameter was about 7.96 μm; further, the distribution appeared to be a bimodal distribution (Figure 3c). In contrast, the size distribution of microcapsules prepared by the T-shaped microchannel was considerably wide, which covered approximately the range from 0.5 to 100 μm (Figure 3b). This was probably due to the unique structure design of the heart-shaped microchannel. As shown in Figure 4a, when the

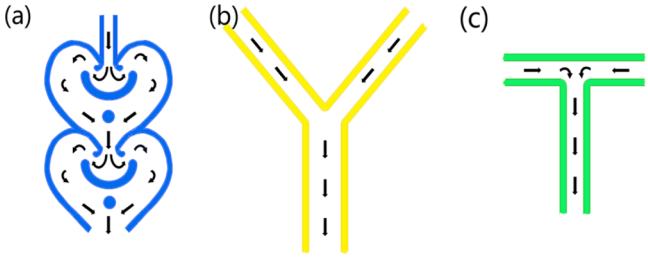

Figure 4. Schematic diagram of the microchannels with different structures: (a) heart-shaped, (b) Y-shaped, and (c) T-shaped.

dispersed- and continuous-phase fluids entered the heart-shaped unit, they were hindered by the U-shaped structure obstacle and split into two streams with different flow directions, after which the two streams flowed along the microchannel wall and converged again near the cylindrical post, flowing into the next heart-shaped unit from the narrow access.[47−50] In this process, the dispersed phase and continuous phase diffused and mixed with each other by splitting and recombining, which was repeated several times in a heart-shaped unit. However, in the T-shaped or Y-shaped unit, the dispersed- and continuous-phase fluids flowed in the different directions and underwent only one collision (Figure 4b,c). Therefore, the application of the heart-shaped microchannel in the microcapsule manufacture had prominent advantages including a uniform dimension and good monodispersity, which is a necessary prerequisite to realize the coincident release of microcapsules.

2.1.2. Effects of the Surfactant. The surfactant can promote the mutual mixing of the dispersed phase and the continuous phase to form a completely dispersed emulsion and can also prevent the aggregation of microcapsules once the shell is formed.[51] In this study, the effects of different types of surfactants including SP-27001 (an ester compound of the styrene maleic anhydride copolymer), 601 (tristyrylphenol ethoxylates), and sodium lignosulfonate on the preparation of pendimethalin microcapsules were explored. Figure 5 shows the stability indices of the emulsions formed by the three surfactants at the same amount of addition. It can be seen from Figure 5a that the Turbiscan stability index (TSI) of the emulsion prepared with sodium lignosulfonate as a surfactant increased dramatically over a time scale of 200 min. It may be explained with the alkalinity of sodium lignosulfonate, which could accelerate the reaction of MDI with water. Figure 5b shows that the stability index of the emulsion only increased by

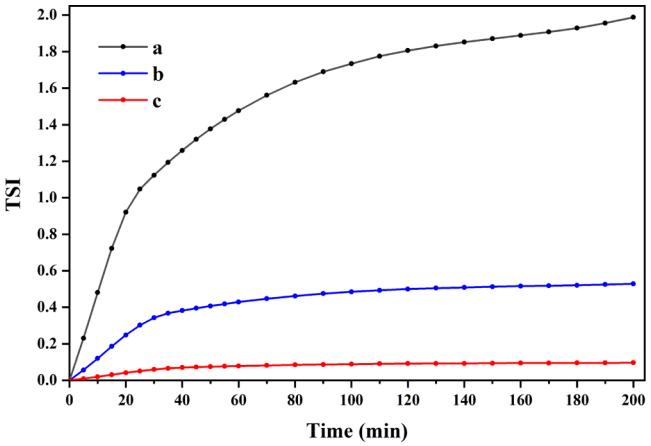

Figure 5. TSIs of the emulsions formed by different types of surfactants: (a) 601, (b) SP-27001, and (c) lignosulfonate.

0.4 within 200 min when surfactant 601 was used, indicating that 601 had a better emulsifying effect than sodium lignosulfonate. However, the agglomeration of microcapsules was discovered during the formation of the shell. The reason for this phenomenon may be that the terminal hydroxyl group of phenol could react with MDI, which affected the synthesis of the polyurea shell and enabled the microcapsules to adhere to each other. As shown in Figure 5c, the TSI of the emulsion in the presence of surfactant SP-27001 increased simply to 0.1 after 200 min, indicating that almost no particle migration or particle size change occurred. This was due to the tremendous advantages of SP-27001 in reducing the surface tension of the system and improving the kinetic stability at the oil−water interface. Specifically, the styrene in the main chain along with the side carbon chain extending into the oil phase could provide the steric hindrance, and the negatively charged hydrolyzed maleic anhydride could provide the electrostatic repulsion, aiding the homogeneous fine emulsified droplets to exist for a long time.[52] Thus, surfactant SP-27001 and polyurea have a good adsorbability and compatibility, which was beneficial to maintain the stability of the emulsion and restrain the fast coalescence of droplets.

2.1.3. Effects of Temperature. Figure 6 shows the biological microscopy images of pendimethalin microcapsules prepared at different reaction temperatures (60, 65, and 70 °C). It is obvious from Figure 6 that all microcapsules had nearly spherical shapes with clear diffraction rings. The appearance of a diffraction ring was due to the difference in the refractive indexes between the external and internal parts of microcapsules, which could preliminarily confirm the generation of the polyurea shell.[14] When the temperature was at 60 °C, some of the pendimethalin was not encapsulated and was distributed outside the microcapsules in the form of a crystal (Figure 6a). This may be due to the low melting point of pendimethalin (56−57 °C), and a lower reaction temperature would make it easier for the core material to crystallize and precipitate when the emulsion comes into contact with the cold EDA aqueous solution in the microchannel. When the temperature was at 70 °C, adhesion of microcapsules was observed, and the uniformity of the microcapsules was deteriorated (Figure 6c). This was probably due to the accelerated thermodynamic diffusion effect, which increased the frequency of collisions between the reactive monomers and speeded up the rate of the polymerization reaction.[45] This suggests that to obtain the

https://doi.org/10.1021/acsomega.1c05903
ACS Omega 2021, 6, 34160−34172

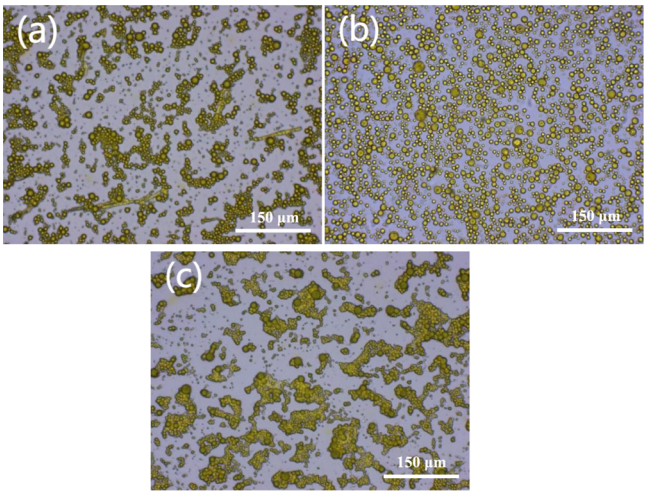

Figure 6. Biological microscopy images of pendimethalin microcapsules prepared at different temperatures: (a) 60, (b) 65, and (c) 70 °C.

desired microcapsules under the above experimental conditions, an appropriate reaction temperature is also necessary.

2.2. Characterization of Pendimethalin Microcapsules. *2.2.1. Fourier Transform Infrared Spectra Analysis.* Figure 7 shows the Fourier transform infrared (FTIR) spectroscopy data of MDI, the polyurea shell, pendimethalin, and pendimethalin microcapsules. It can be seen from Figure 7a that MDI had a strong characteristic peak at 2279 cm^{-1} due to the presence of −N═C═O. As shown in Figure 7b, the absorption peak appearing at around 1635 cm^{-1} was ascribed to the stretching vibration of C═O, the peak appearing at 3432 cm^{-1} was ascribed to the stretching vibration of N−H, and the peaks at 1087 and 1049 cm^{-1} were attributed to the C−N stretching vibration of amide and aromatic groups.[23,43] These results could prove the formation of the urea linkage between isocyanate and amine groups. Moreover, the −N═C═O absorption peak disappeared in the spectrum, which could also verify the synthesis of the polyurea shell. The absorption peak appearing at 3428 cm^{-1} was assigned to the stretching vibration of N−H, the peaks at 1536 and 1380 cm^{-1} were assigned to the stretching vibration of $-NO_2$, and the peaks at 1248 and 1187 cm^{-1} belonged to the C−N stretching vibration of pendimethalin (Figure 7c).[41] These characteristic peaks could still be seen in the infrared spectrum of pendimethalin microcapsules, and no new bands were observed (Figure 7d), indicating that pendimethalin was successfully encapsulated in the microcapsules and no reaction between the pendimethalin and shell materials occurred.

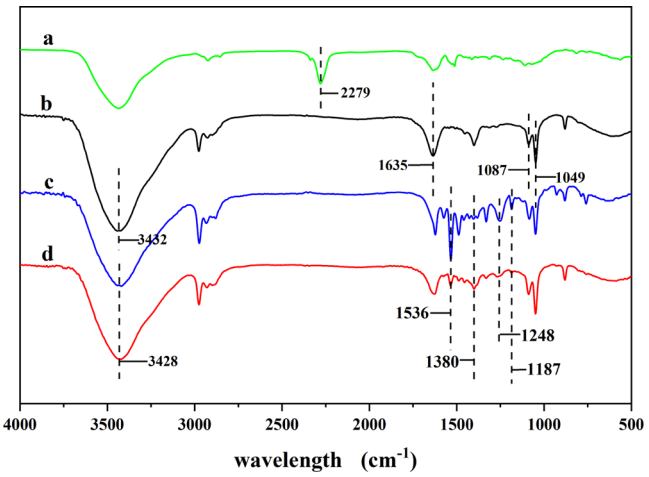

Figure 7. FTIR spectra of MDI (a), polyurea shell (b), pendimethalin (c), and pendimethalin microcapsules (d).

2.2.2. Thermogravimetric Analysis. Figure 8 shows the thermogravimetric analysis (TGA) curves of pendimethalin, the polyurea shell, and pendimethalin microcapsules prepared with different flow rates of the EDA aqueous solution (Q_s). As shown in Figure 8a, pendimethalin began to degrade and evaporate at about 180 °C, and the weight loss ratio approached 100% at approximately 305 °C. Similar results were also found in the previous research studies.[12,14,38] For the polyurea outer shell, the weight loss mainly included two stages with around 30% of the original weight remaining at 800 °C, which could prove the excellent thermal stability of the shell. The slight weight loss in the first stage between 110 and 200 °C was due to the degradation of the unreacted shell materials, and the second decomposition stage above 320 °C was attributed to the degradation of polyurea.

It can be seen that the curve profiles of pendimethalin microcapsules highly overlap each other, indicating that they had the same components and similar structures. The microcapsules experienced weight loss in three important stages with the increase in temperature. The first stage below 185 °C corresponded to the evaporation of water and the decomposition of polyurea shell materials. The second substantial weight loss observed between 185 and 315 °C was attributed to the decomposition and evaporation of pendimethalin, and the relative content of pendimethalin in the microcapsules was approximately 65%. The third stage above 320 °C was ascribed to the degradation of the residual polyurea outer shell, and there were still some residues left (with weight loss values of 7.48%, 10.17%, and 14.68%, as shown in Figure 8c−e, respectively) after 800 °C. This may suggest that the EDA aqueous solution with a higher flow rate could make the shells of pendimethalin microcapsules thicker.

2.3. Size and Morphology Control of Pendimethalin Microcapsules. The size of microcapsules is one of the crucial factors imposing a paramount effect on the release behavior and application performance of loaded pesticides. According to the existing studies, the particle size of the microcapsules was bound up with the flow rates of the continuous phase and dispersed phase, which are recognized as tunable parameters during the preparation in a microfluidic device.[24,53] Here, we focused our investigation on the effects of Q_c (the flow rate of the continuous phase) on the particle size of pendimethalin microcapsules. As shown in Figure 9, the mean diameter of microcapsules increased with the increase in Q_c. This was because when the flow rate of the continuous phase was higher, the isocyanate was more readily converted to amine under the action of water during the emulsion formation process. Although the reaction between isocyanate and water was very slow, the resultant amine could promptly polymerize with isocyanate before the tiny emulsified droplets were fully formed. This polymerization started from the surface of the droplet by forming a polyurea film first, and once the film was formed, the size of the microcapsule was basically fixed.[45] To make the particle size of the microcapsules as small as possible, we continued reducing Q_c while other experimental conditions were kept constant. However, when Q_c was less than 3 mL/

https://doi.org/10.1021/acsomega.1c05903
ACS Omega 2021, 6, 34160−34172

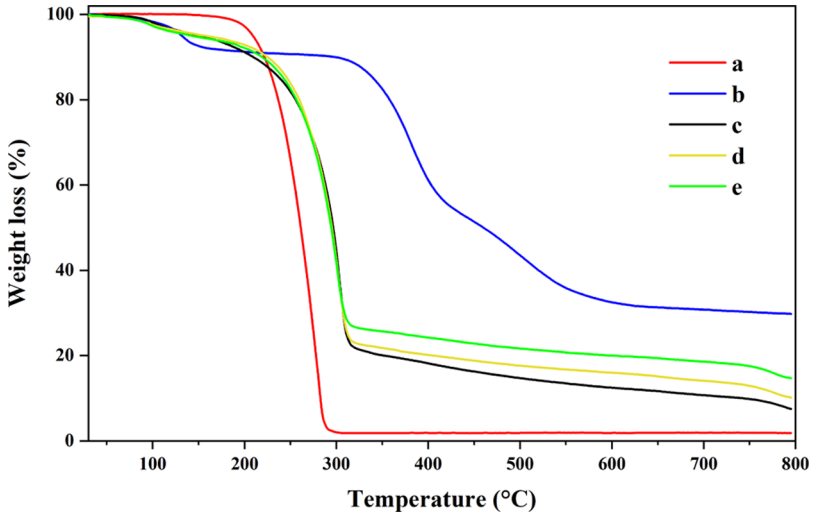

Figure 8. TGA curves of pure pendimethalin (a), polyurea shell (b), and pendimethalin microcapsules with different Q_s values of (c) 0.3, (d) 0.5, and (e) 1.0 mL/min.

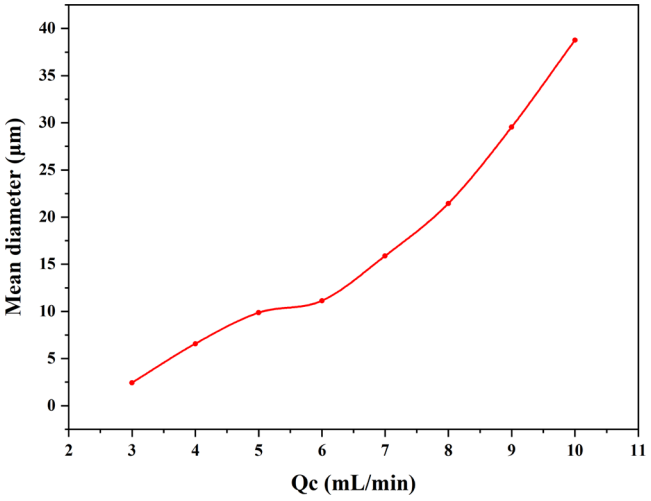

Figure 9. Effects of Q_c on the particle size of pendimethalin microcapsules for Q_d = 5 mL/min and Q_s = 0.5 mL/min.

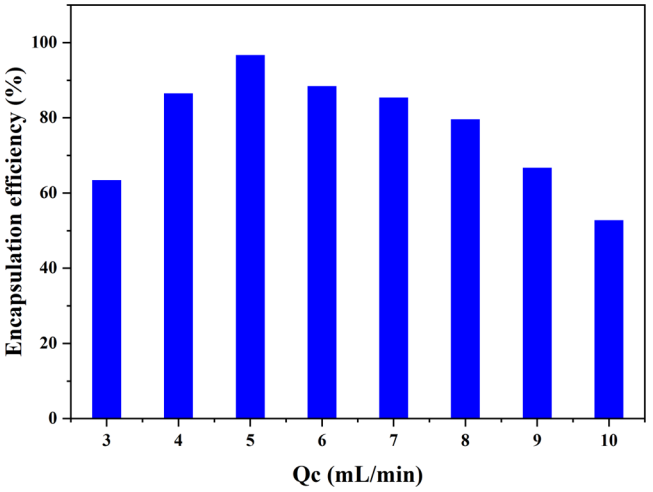

Figure 10. Encapsulation efficiency of pendimethalin microcapsules prepared with different Q_c values for Q_d = 5 mL/min and Q_s = 0.5 mL/min.

min, it was difficult to obtain stable O/W emulsified droplets due to the weakened squeeze and shear action of the continuous phase on the dispersed phase, and no microcapsules were obtained as a consequence.

Figure 10 shows the relationship between the encapsulation efficiency of pendimethalin microcapsules and the flow rate of the continuous phase flow rate, Q_c. When Q_c was changed from 3 to 5 mL/min, the encapsulation efficiency of microcapsules increased from 63.4 to 96.7%. However, when Q_c was more than 5 mL/min, the encapsulation efficiency of microcapsules gradually decreased with the increase in Q_c. This tendency was correlated with the loss of pendimethalin in the dispersed phase. On one hand, when the flow rate of the continuous phase was in a lower range, pendimethalin became hard to disperse in the continuous phase and quickly settled down due to the lack of water and the surfactant.[6,38] On the other hand, when the flow rate of the continuous phase was in a higher range, more pendimethalin was dissolved in water, and the concentration of the active ingredient in the dispersed phase was comparatively low. In both cases, the reduction of pendimethalin would ultimately cause an unsatisfactory drug loading and encapsulation efficiency of the microcapsules.

For the range of parameters explored, microcapsules were produced with a mean diameter ranging from 2.43 to 38.76 μm. This result indicated that within the range of the operable parameters for generating the stable emulsion, it was feasible and practical to accurately control the particle size of microcapsules by changing the flow rate of the continuous phase. However, too fast and too slow flow rates of the continuous phase would both reduce the encapsulation efficiency, which certainly decreased the production efficiency of the microcapsule preparation technology. To balance the size and encapsulation efficiency of microcapsules, we chose the continuous phase flow rate of 5 mL/min for further research.

It is important to mention that the effects of the Q_s on the particle size of pendimethalin microcapsules were also examined, while the variation was slight. The mean diameters of the microcapsules prepared with Q_s values of 0.3, 0.5, 1.0, and 2.0 mL/min were 9.18 m, 9.54 m, 9.37, and 9.44 μm, respectively, suggesting that the flow rate of the EDA aqueous

https://doi.org/10.1021/acsomega.1c05903
ACS Omega 2021, 6, 34160−34172

solution had no considerable influence on the microcapsule size. This was reasonable because the size of the microcapsule was proportional to the corresponding emulsified droplet size. The emulsion had been basically formed in microchannel I, which was supposed to be wrapped in microchannel II. Thus, the EDA solution subsequently added could hardly affect the size of the microcapsules. However, the morphologies of the microcapsules produced with different Q_s values were significantly different. This was because the flow rate of Q_s determined the ratio of hydrophilic monomer EDA and lipophilic monomer MDI, which affected the polymerization reaction of the polyurea shell.

Figure 11 shows the scanning electron microscopy (SEM) images of pendimethalin microcapsules with different Q_s

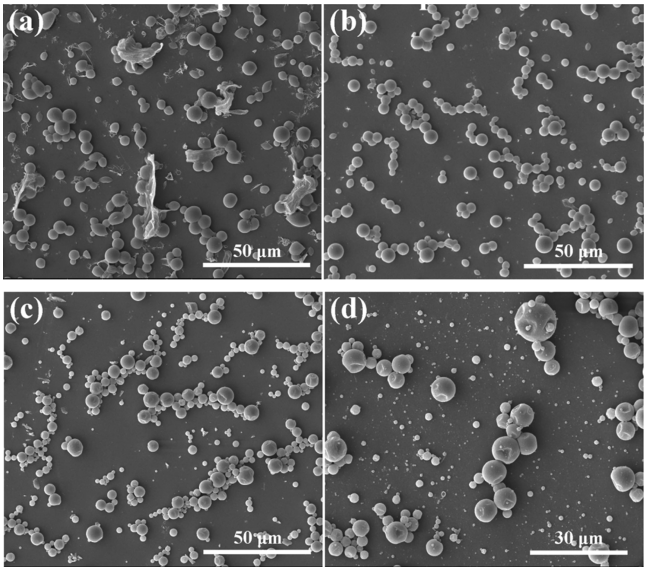

Figure 11. SEM images of pendimethalin microcapsules prepared with different Q_s values of (a) 0.3, (b) 0.5, (c) 1.0, and (d) 2.0 mL/min.

values. When Q_s was 0.3 mL/min, a large number of microcapsules appeared with irregular shapes, and some pendimethalin had leaked out from the microcapsules (Figure 11a). This was mainly due to the insufficient EDA amount. In this case, the outer shell of the microcapsules was too thin to completely cover the core moiety due to the lack of shell materials, leading to the fragile structure and poor mechanical properties. Meanwhile, the formation of the polyurea shell might be dominated by the reaction between MDI and water, producing more CO_2 and forming pores on the shell surface,[45] which was beyond the scope of this research. When Q_s was increased to 0.5 mL/min, the microcapsules had regular spherical shapes with a smooth surface and high uniformity (Figure 11b), which was conductive to the construction of efficient controlled release formulation. As shown in Figure 11c, a small proportion of the microcapsules presented slight wrinkles when Q_s was 1.0 mL/min (Figure 11c). The appearance of wrinkles resulted from the reduction of the internal core volume caused by MDI being consumed in a short time.[44] However, when Q_s reached 2.0 mL/min, most of the microcapsules had big dimples and collapses (Figure 11d). Another typical phenomenon observed was the adhesion of microcapsules. This was attributed to excess EDA. At this high concentration of EDA, the reaction between MDI and EDA was greatly enhanced, and the degrees of shrinkage and collapse were further increased, which was responsible for the tendency of microcapsules to coalesce with each other and thereby reduced their dispersion.[46]

These results highlighted the importance of EDA in determining the shell morphology of the resulting pendimethalin microcapsules. This demonstrated that the morphology of the pendimethalin microcapsules could be changed by changing the flow rate the EDA aqueous solution, while the flow rates of the continuous phase and dispersed phase were kept constant.

2.4. Sustained Release of Pendimethalin Microcapsules. To explore the release behaviors of pendimethalin microcapsules with different morphologies, the microcapsules fabricated under different Q_s values (0.3, 0.5, 1.0, and 2.0 mL/min) were selected for the sustained release experiment. Figure 12 shows the cumulative release proportions of pendimethalin

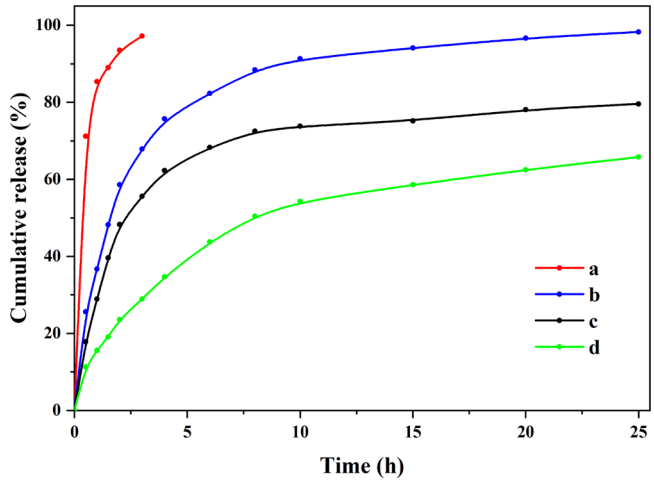

Figure 12. Cumulative release proportions of pendimethalin microcapsules prepared with different Q_s values of (a) 0.3, (b) 0.5, (c) 1.0, and (d) 2.0 mL/min.

microcapsules. It was found that the release rate of pendimethalin from the microcapsules decreased with the increase in Q_s. In particular, the microcapsules prepared with a Q_s of 0.3 mL/min exhibited a burst release at the beginning (Figure 12a). More than 71.2% pendimethalin was released from microcapsules within 0.5 h, and the cumulative release rate was up to 97.2% after 3 h. This was because the polyurea shell formed in this case was very thin and fragile, contributing to the permeation and effusion of the active ingredient from the microcapsules. For the remaining three microcapsules, the release curves of pendimethalin could be divided into two stages, the first stage of initial rapid release, followed by the second stage of relatively slow release, suggesting that all of them possessed the behavior of controlled and sustained release. As shown in Figure 12b, the cumulative release proportion for the microcapsules prepared with a Q_s of 0.5 mL/min was 67.9% at 10 h and reached 98.3% after 25 h. By comparison, the cumulative release proportions for the microcapsules prepared with a Q_s of 1.0 and 2.0 mL/min were 55.6 and 28.9% at 10 h and only reached 72.1 and 62.5% after 25 h, respectively (Figure 12c,d). This may be because the higher feeding rate of the EDA aqueous solution may accelerate the reaction of MDI with EDA, facilitating the deposition of polyurea on the surface to make the shell

https://doi.org/10.1021/acsomega.1c05903
ACS Omega 2021, 6, 34160−34172

rougher,[22] which needs a further proof. Furthermore, the adhesion of microcapsules could reduce the contact area with the release medium and hinder the release process of the active ingredient, thus leading to the slowest release rate of the microcapsules prepared with a Q_s of 2.0 mL/min. These variations in release behaviors were largely due to significant differences in the surface morphologies of the microcapsules prepared with different Q_s values.

Figure 13 shows the biological microscopy images of pendimethalin microcapsules in the release medium. As

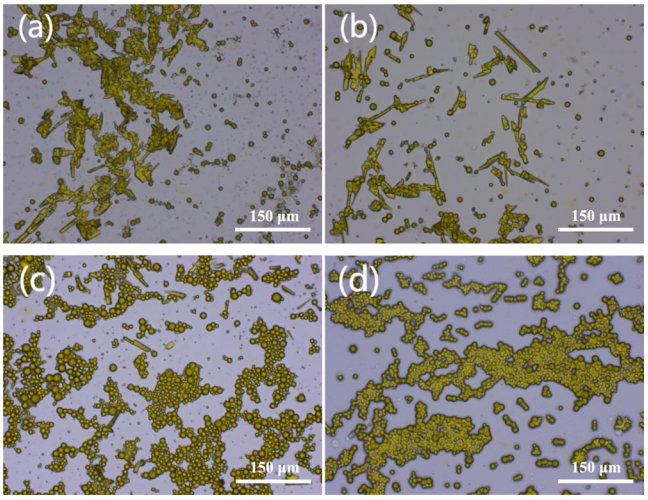

Figure 13. Biological microscopic observation of pendimethalin microcapsules prepared with different Q_s values of (a) 0.3, (b) 0.5, (c) 1.0, and (d) 2.0 mL/min.

shown in Figure 13a, lots of crystals could be seen in the release medium, suggesting that most pendimethalin had released from the microcapsules prepared with a Q_s of 0.3 mL/min. It can be clearly seen from Figure 13d that a huge number of microcapsules with a Q_s of 2.0 mL/min were coalesced in a chunk, and nearly no pendimethalin was released as a consequence. Comparatively, when Q_s values were 0.5 and 1.0 mL/min, pendimethalin was released from the microcapsules at moderate rates (Figure 13b,c). These results were in good agreement with the cumulative release curses of microcapsules.

It could be concluded that the release behavior of pendimethalin could be regulated by the surface morphology of microcapsules, which was controlled by varying the flow rate of the EDA aqueous solution. This may provide valuable information for the direction of sustained release control in microcapsules from another perspective.

2.5. Bioassay of Pendimethalin Microcapsules. Table 2 shows the stem control efficacy of pendimethalin microcapsules prepared with different Q_s values against grassy weeds and broad-leaf weeds at the same concentration. It was considered that the herbicidal activity results were associated with the surface morphology and release characteristics of the microcapsules mentioned above. The microcapsules prepared with a Q_s of 0.3 mL/min exhibited similar herbicidal effects to the pendimethalin EC. Despite the stem control efficacy for grassy weeds of as high as 95.03%, the stem control efficacy of microcapsules for broad-leaf weeds was simply 41.27% because of the premature release. Among all samples, the microcapsules prepared with a Q_s of 0.5 mL/min had the best herbicidal

Table 1. Stem Control Efficacy of Pendimethalin Microcapsules Prepared with Different Q_s Values against Grassy Weeds and Broad-Leaf Weeds (0.3 mL/min, 0.5 mL/min, 1.0 mL/min, and 2.0 mL/min)

	grassy weeds		broad-leaf weeds	
treatment	average plant number	stem control efficacy (%)	average plant number	stem control efficacy (%)
A	36.0	95.03a	78.7	41.27b
B	51.3	92.91a	36.3	72.91a
C	93.0	87.15ab	40.0	70.15a
D	511.3	29.38b	84.3	37.08b
EC	52.7	92.72a	82.0	38.81b
blank control	724.0		134.0	

Table 2. Total Stem Control Efficacy and Fresh Weight Reduction of Pendimethalin Microcapsules Prepared with Different Q_s Values against Weeds (0.3 mL/min, 0.5 mL/min, 1.0 mL/min, and 2.0 mL/min)

treatment	total plant number	stem control efficacy (%)	fresh weight (g)	fresh weight reduction (%)
A	114.7	86.63a	4.74	87.86a
B	87.7	89.78a	3.81	90.24a
C	133.0	84.49a	5.40	86.17a
D	595.7	30.57b	26.18	32.96b
EC	134.7	84.30a	5.89	84.92a
blank control	858.0		39.05	

activity. In this case, the stem control efficacies against grassy weeds and broad-leaf weeds were 89.78 and 90.24%, respectively, indicating that the microcapsules could maintain a longer effective duration than the pendimethalin EC. It is worth noting that although the release time was the longest, the herbicidal effect of the microcapsules prepared with a Q_s of 2.0 mL/min was the worst. The reason for this may be that pendimethalin was used as a pre-emergence herbicide in the experiments, which mainly acted during the germination of seeds and could not kill weeds that had already grown out of the ground.[39] This means that an excessively slow release rate of microcapsules would cause the pendimethalin to miss the critical period for weed control.

Table 2 shows the total stem control efficacy and fresh weight reduction of pendimethalin microcapsules prepared with different Q_s values against weeds at the same concentration. It is obvious that the total stem control efficacy and fresh weight reduction of pendimethalin microcapsules were comparable to that of the pendimethalin EC. However, the stem control efficacy of pendimethalin microcapsules against broad-leaf weeds when Q_s was 0.5 or 1.0 mL/min was much higher than that of the pendimethalin EC (Table 1). Furthermore, microcapsules are more environmentally friendly because they can avoid the use of toxic organic solvents. Hence, as an innovative controlled release formulation, pendimethalin microcapsules possess great potential and could replace the use of the pendimethalin EC in agricultural application.

In this study, we found that the flow rate of the EDA aqueous solution could affect the surface morphology of the polyurea shell and further regulate the application performance including the release behavior and herbicidal activity of the

https://doi.org/10.1021/acsomega.1c05903
ACS Omega 2021, 6, 34160−34172

encapsulated pendimethalin, which could act as a useful reference for the design of pesticide microcapsules so as to meet various application requirements.

3. CONCLUSIONS

In this work, pendimethalin microcapsules were developed via the interfacial polymerization of MDI and EDA in a simple microfluidic device. The pendimethalin microcapsules prepared under appropriate conditions had a smooth surface, good monodispersity, high encapsulation efficiency, and excellent thermal stability. The size and morphology control of the produced microcapsules could be achieved by changing the value of Q_d (the flow rate of the dispersed phase) and Q_s. The release behavior of microcapsules was closely related to the morphology of microcapsules. The herbicidal activity of pendimethalin microcapsules depended on the release of the active ingredient. This paper will provide a reference for the application of microfluidics in the preparation and characteristic regulation of pesticide microcapsules.

4. MATERIALS AND METHODS

4.1. Materials. Pendimethalin (purity 98.5%) was supplied by Shandong Binnong Technology Co., Ltd. (Shandong, China). Lipophilic monomer MDI was purchased from Wanhua Chemical Group Co., Ltd. (Shandong, China). Hydrophilic monomer EDA and protective colloid polyvinyl alcohol (PVA) were purchased from Sinopharm Chemical Reagent Co., Ltd. (Beijing, China). Methanol and *n*-hexane were obtained from Shanghai Aladdin Biochemical Technology Co., Ltd. (Shanghai, China). Surfactant SP-27001 (an ester compound of the styrene maleic anhydride copolymer), 601, sodium lignosulfonate, and the commercial pendimethalin EC (330 g/L) were kindly provided by Jiangsu Qingyu Chemical Technology Co., Ltd. (Jiangsu, China). The deionized water used in all experiments was prepared by a distillation device.

4.2. Methods. *4.2.1. Experimental Setup.* The preparation process of pendimethalin microcapsules was completed in a simple microfluidic device, which was divided into a feeding system and a microchannel reaction system. The feeding system consisted of three independent plunger pumps, and the microchannel reaction system consisted of two connected microchannel modules. The microfluidic flow structure was composed of a dispersed-phase fluid (pendimethalin and MDI), a continuous-phase fluid (the surfactant and PVA aqueous solution), and an EDA aqueous solution fluid, which were supplied by plunger pumps above at desired flow rates. The emulsion formation and shell generation process were separated in the two microchannel modules, namely, microchannel I and microchannel II. Briefly, the dispersed-phase and continuous-phase fluids were injected into microchannel I for the formation of emulsified droplets in water, and the EDA aqueous solution fluid was injected into microchannel II to initiate the interfacial polymerization as the emulsion flowed in.

The Microchannel I normally used was a series of heart-shaped units (corning advanced-flow reactor G1 fluidic module) with a nozzle size of 100 μm and a height of 120 μm, which were made of glass. Y-shaped or T-shaped units 100 μm in width and 150 μm in height were used as an alternative when the effects of the microchannel structure on the preparation of microcapsules were explored in the experiment, which were composed of Hastelloy. The microchannel II used comprised tubing with a diameter of 500 μm, which was made of stainless steel.

4.2.2. Preparation of Pendimethalin Microcapsules. The pendimethalin microcapsules were prepared by an interfacial polymerization method, in which an O/W emulsion was used as a template, MDI was used as the first reactant, and EDA was used as the second curing agent to generate the polyurea outer shell. For a typical run, 5 g of PVA and 5 g of surfactant SP-27001 were dissolved in 90 g of deionized water at 90 °C to obtain the continuous phase. Then, 100 g of pendimethalin was heated to 60 °C for complete melting and uniformly mixed with 5 g of MDI to obtain the dispersed phase. Both the continuous and dispersed phases were placed in a water thermostat bath at 60 °C for further use. As for the EDA aqueous solution, 10 g of EDA was dissolved in 90 g of deionized water and placed in a water thermostat bath at 20 °C.

In this method, MDI and EDA quickly reacted at the oil−water surface of the emulsion and formed solid polyurea shells around the emulsified droplets. However, because of the high reactivity of MDI and EDA, the shell could immediately generate even before the droplets were completely formed, resulting in the clogging of the microchannel.[44] To overcome this problem, the dispersed phase containing MDI and the continuous phase were injected into microchannel I through two plunger pumps, and the EDA aqueous solution was injected into microchannel II through another plunger pump, as mentioned above. The flow rates of the continuous phase (Q_c), the dispersed phase (Q_d), and the EDA aqueous solution (Q_s) were optimized to be 5, 5, and 0.5 mL/min, respectively. The temperature of the microfluidic device was kept at 65 °C, and the residence time of fluids in the microchannel was 30 min. After the completion of the shell growth, the produced microcapsules were gently collected by a glass container. Then, the microcapsules were washed twice with deionized water and dried in vacuum at room temperature to remove the water. The microcapsules were further placed overnight in an oven at 45 °C to evaporate the vast majority of the water if a dried sample was required in the characterization. It is to be noted that the final obtained pendimethalin microcapsule product was in the form of an aqueous suspension, and no organic solvent was used in the preparation process. Pendimethalin returns to the crystal state as the temperature is decreased and is still well-encapsulated in the firm polyurea shells.

By means of the microfluidic technology, the manufacture of pendimethalin microcapsules can be easily and continuously performed for several hours. Since the formed emulsion could remain stable over a wide range of process parameters, the flow rates of the continuous phase and the EDA aqueous solution were finely adjusted to prepare microcapsules with varying sizes and morphologies. In addition, different types of surfactants and microchannels were also used for the preparation of microcapsules to optimize the production conditions.

4.2.3. Characterization of Pendimethalin Microcapsules. The chemical structures of the raw materials and prepared pendimethalin microcapsules were analyzed with an FTIR spectrometer (VERTEX 80 V, Bruker, Germany) at room temperature by using compressed potassium bromide (KBr) discs. The scanning range of the infrared spectrometer was 4000−500 cm^{-1} with 32 scans per spectrum, and the resolution was 4.0 cm^{-1}. The TSI of the emulsions, which

https://doi.org/10.1021/acsomega.1c05903
ACS Omega 2021, 6, 34160−34172

represents the kinetic stability of the system, was measured by a stability analyzer (Turbiscan LAB, FORMULACTION, France).

The surface morphology of the pendimethalin microcapsules was observed via a biological microscope (BM2000, Nanjing Jiangnan Novel Optics Co., Ltd, China) and a scanning electron microscope (EM-30Plus, COXEM, Korea). The mean particle size and size distribution of the pendimethalin microcapsules were determined by a laser diffraction particle size analyzer (Bettersize2600, Dandong Baxter Instrument Co., Ltd, China). The thermal stability of the pendimethalin microcapsules was measured by a thermogravimetric analyzer (TGA 4000, Shanghai Innuo Precision Instrument Co., Ltd, China) at a heating rate of 20 °C/min under a nitrogen atmosphere (20 mL/min) from 30 to 805 °C.

4.2.4. Determination of the Encapsulation Efficiency. During the formation of microcapsules, a small amount of pendimethalin may dissolve in the water, and thereby, the encapsulation efficiency of pendimethalin microcapsules obtained is actually not 100%, which could be calculated by measuring the content of free pendimethalin. First, 0.5 g of the pendimethalin microcapsule sample was weighed and dissolved in 30 mL of methanol in a beaker. The solution was transferred to a volumetric flask and diluted to 50 mL with methanol. The supernatant of the sample was collected after sonication and centrifuging, which contained all the pendimethalin in the sample. Then, 0.5 g of the pendimethalin microcapsule sample prepared under the same conditions was also weighed and dissolved according to the same procedure described above. The supernatant of the sample was collected after centrifuging without sonication, which contained the free pendimethalin in the sample. The content of pendimethalin in the supernatant was determined by using a high-performance liquid chromatography (HPLC) equipment (LC-20AD, Shimadzu, Japan) equipped with an ultraviolet (UV) detector.

The wavelength of the UV detector was set to be 230 nm. The chromatographic separation was carried out by a stainless-steel column (250 mm × 4.6 mm, 5 μm) filled with Zorbax ODS, and the column temperature was set at room temperature. The mobile phase was a mixture of methanol and water (90:10, v/v) with a flow rate of 1.0 mL/min, and the injection volume was 5 μL. The total amount and the free content of pendimethalin could be confirmed based on the known standard absorption curve.

The encapsulation efficiency was calculated according to eq 1, where C_1 is the total amount of pendimethalin and C_2 is the content of free pendimethalin

$$\text{encapsulation efficiency}(\%) = \frac{C_1 - C_2}{C_1} \times 100 \quad (1)$$

4.2.5. Sustained Release Experiment. The release characteristics of pendimethalin microcapsules were measured according to a reported method with minor modifications.[41] Typically, 0.1 g of the dried pendimethalin microcapsule sample was weighed and transferred to a 250 mL flask, and 100 mL of an *n*-hexane/methanol mixture (90:10, v/v) was added as a release medium. The solution was kept at 30 °C and stirred at a rate of 400 rpm. The same volume of a fresh release medium was supplemented immediately when 0.5 mL of the sample solution was taken out from the flask at different time intervals (0.5, 1, 1.5, 2, 3, 4, 6, 8, 10, 15, 20, and 25 h). The pendimethalin content of the sample solution and total concentration of the dried sample were analyzed by HPLC, as described above in Section 4.2.4.

The cumulative release proportion was calculated according to eq 2, where C_0 is the total amount of pendimethalin in the sample and C_t is the content of pendimethalin in the release medium at a certain moment

$$\text{cumulative release proportion}(\%) = \frac{C_t}{C_0} \times 100 \quad (2)$$

4.2.6. Herbicidal Activity Experiment. The herbicidal activity of pendimethalin microcapsules against grass and broad-leaf weeds was evaluated in an indoor culture experiment. The target weeds selected for testing included *Poa annua* L., *Lolium perenne* L., and *Polygonum lapathifolium* L. Briefly, air-dried and sieved topsoil was thoroughly mixed with sphagnum peat (organic matter content: 2.1% and N, P, and K content: 0.25%) in a particular proportion (90:30, w/w) to obtain a soil mixture. Certain numbers of weed seeds were sown evenly in a square pot (40 cm × 40 cm) containing the soil mixture with the proper quantity. In the weed control experiments, four microcapsule samples prepared with different Q_s values (0.3, 0.5, 1.0, and 2.0 mL/min) and the commercial pendimethalin EC were diluted 400 times with deionized water and applied to the surface of the mixed soil by spraying soon after the planting. The same amount of deionized water was also sprayed as a blank control. All pots were placed indoors to receive light (14 h/10 h, L/D) and kept under the conditions of 25−30 °C and around 60% relative humidity. The pH of the soil was controlled to be between 7.0 and 7.5, and each pot was irrigated by naturally absorbing water from the bottom. Thirty days after the treatment, the surviving weeds were cut off with scissors along the surface of the soil. The numbers of plants were recorded, and the weight of the weeds was obtained to calculate the effects of the active ingredient on the weeds. Each treatment was repeated three times in a completely randomized design.

The stem control efficacy was calculated according to eq 3, where N_1 and N_0 represent the numbers of plants in the treatment and blank control, respectively

$$\text{stem control efficacy}(\%) = \frac{N_0 - N_1}{N_0} \times 100 \quad (3)$$

The fresh weight reduction was calculated according to eq 4, where W_1 and W_0 represent the total fresh weights of the plants in the treatment and blank control, respectively

$$\text{fresh weight reduction}(\%) = \frac{W_0 - W_1}{W_0} \times 100 \quad (4)$$

AUTHOR INFORMATION

Corresponding Author

Xiaoli Gu − *Co-Innovation Center for Efficient Processing and Utilization of Forest Products, College of Chemical Engineering, Nanjing Forestry University, Nanjing 210037, P. R. China;* orcid.org/0000-0001-8588-0358; Email: guxiaoli@njfu.edu.cn

Authors

Yu Qin − *Co-Innovation Center for Efficient Processing and Utilization of Forest Products, College of Chemical Engineering, Nanjing Forestry University, Nanjing 210037, P. R. China*

https://doi.org/10.1021/acsomega.1c05903
ACS Omega 2021, 6, 34160−34172

Xinyu Lu − *Co-Innovation Center for Efficient Processing and Utilization of Forest Products, College of Chemical Engineering, Nanjing Forestry University, Nanjing 210037, P. R. China*

Han Que − *Co-Innovation Center for Efficient Processing and Utilization of Forest Products, College of Chemical Engineering, Nanjing Forestry University, Nanjing 210037, P. R. China*

Dandan Wang − *Co-Innovation Center for Efficient Processing and Utilization of Forest Products, College of Chemical Engineering, Nanjing Forestry University, Nanjing 210037, P. R. China*

Tao He − *Co-Innovation Center for Efficient Processing and Utilization of Forest Products, College of Chemical Engineering, Nanjing Forestry University, Nanjing 210037, P. R. China*

Dingxiang Liang − *Co-Innovation Center for Efficient Processing and Utilization of Forest Products, College of Chemical Engineering, Nanjing Forestry University, Nanjing 210037, P. R. China*

Xu Liu − *Co-Innovation Center for Efficient Processing and Utilization of Forest Products, College of Chemical Engineering, Nanjing Forestry University, Nanjing 210037, P. R. China*

Jiajia Chen − *Co-Innovation Center for Efficient Processing and Utilization of Forest Products, College of Chemical Engineering, Nanjing Forestry University, Nanjing 210037, P. R. China*

Chenrong Ding − *Co-Innovation Center for Efficient Processing and Utilization of Forest Products, College of Chemical Engineering, Nanjing Forestry University, Nanjing 210037, P. R. China*

Pengcheng Xiu − *Co-Innovation Center for Efficient Processing and Utilization of Forest Products, College of Chemical Engineering, Nanjing Forestry University, Nanjing 210037, P. R. China*

Chaozhong Xu − *Co-Innovation Center for Efficient Processing and Utilization of Forest Products, College of Chemical Engineering, Nanjing Forestry University, Nanjing 210037, P. R. China;* orcid.org/0000-0002-3467-4244

Complete contact information is available at: https://pubs.acs.org/10.1021/acsomega.1c05903

Author Contributions

Conceptualization, Y.Q.; methodology, X.L. and H.Q.; software, X.L., J.C., C.D., and P.X.; validation, D.W., D.L., and T.H.; formal analysis, C.X.; investigation, X.G.; resources, X.G.; data curation, Y.Q.; writing−original draft preparation, Y.Q.; writing−review and editing, X.G.; visualization, X.G.; supervision, X.G.; project administration, C.X.; and funding acquisition, X.G. All authors have read and agreed to the published version of the manuscript.

Notes

The authors declare no competing financial interest.

■ ACKNOWLEDGMENTS

This research was supported by financial support from the National Natural Science Foundation of China (no. 21774059), the Priority Academic Program Development (PAPD) of Jiangsu Higher Education Institutions, and the opening funding of Jiangsu Key Lab of Biomass-based Green Fuels and Chemicals.

■ REFERENCES

(1) Liu, B.; Wang, Y.; Yang, F.; Wang, X.; Shen, H.; Cui, H.; Wu, D. Construction of a controlled-release delivery system for pesticides using biodegradable PLA-based microcapsules. *Colloids Surf., B* **2016**, *144*, 38−45.

(2) Zheng, L.; Cao, C.; Cao, L.; Chen, Z.; Huang, Q.; Song, B. Bounce Behavior and Regulation of Pesticide Solution Droplets on Rice Leaf Surfaces. *J. Agric. Food Chem.* **2018**, *66*, 11560−11568.

(3) Zhang, Y.; Liu, B.; Huang, K.; Wang, S.; Quirino, R. L.; Zhang, Z.-x.; Zhang, C. Eco-Friendly Castor Oil-Based Delivery System with Sustained Pesticide Release and Enhanced Retention. *ACS Appl. Mater. Interfaces* **2020**, *12*, 37607−37618.

(4) Lyons, S. M.; Hageman, K. J. Foliar Photodegradation in Pesticide Fate Modeling: Development and Evaluation of the Pesticide Dissipation from Agricultural Land (PeDAL) Model. *Environ. Sci. Technol.* **2021**, *55*, 4842−4850.

(5) Patil, D. K.; Agrawal, D. S.; Mahire, R. R.; More, D. H. Synthesis, characterization, and controlled release study of polyurea microcapsules containing metribuzin herbicide. *Russ. J. Appl. Chem.* **2016**, *88*, 1692−1700.

(6) Liu, B.; Wang, Y.; Yang, F.; Cui, H.; Wu, D. Development of a Chlorantraniliprole Microcapsule Formulation with a High Loading Content and Controlled-Release Property. *J. Agric. Food Chem.* **2018**, *66*, 6561−6568.

(7) Sefiloglu, F. O.; Tezel, U.; Balcıoğlu, I. A. Validation of an Analytical Workflow for the Analysis of Pesticide and Emerging Organic Contaminant Residues in Paddy Soil and Rice. *J. Agric. Food Chem.* **2021**, *69*, 3298−3306.

(8) Wu, T.; Fang, X.; Yang, Y.; Meng, W.; Yao, P.; Liu, Q.; Zhang, B.; Liu, F.; Zou, A.; Cheng, J. Eco-friendly Water-Based λ-Cyhalothrin Polydopamine Microcapsule Suspension with High Adhesion on Leaf for Reducing Pesticides Loss. *J. Agric. Food Chem.* **2020**, *68*, 12549−12557.

(9) Luo, J.; Huang, X.-p.; Jing, T.-f.; Zhang, D.-x.; Li, B.; Liu, F. Analysis of Particle Size Regulating the Insecticidal Efficacy of Phoxim Polyurethane Microcapsules on Leaves. *ACS Sustain. Chem. Eng.* **2018**, *6*, 17194−17203.

(10) Wang, Y.; Li, C.; Wang, T.; Li, X.; Li, X. Polylactic Acid-Graphene Oxide-based Materials for Loading and Sustained Release of Poorly Soluble Pesticides. *Langmuir* **2020**, *36*, 12336−12345.

(11) Xu, C.; Cao, L.; Zhao, P.; Zhou, Z.; Cao, C.; Zhu, F.; Li, F.; Huang, Q. Synthesis and Characterization of Stimuli-Responsive Poly(2-dimethylamino-ethylmethacrylate)-Grafted Chitosan Microcapsule for Controlled Pyraclostrobin Release. *Int. J. Mol. Med.* **2018**, *19*, 854−868.

(12) Hedaoo, R. K.; Mahulikar, P. P.; Gite, V. V. Synthesis and Characterization of Resorcinol-Based Cross Linked Phenol Formaldehyde Microcapsules for Encapsulation of Pendimethalin. *Polym. Plast. Technol. Eng.* **2013**, *52*, 243−249.

(13) Yuan, H.; Li, G.; Yang, L.; Yan, X.; Yang, D. Development of melamine-formaldehyde resin microcapsules with low formaldehyde emission suited for seed treatment. *Colloids Surf., B* **2015**, *128*, 149−154.

(14) Hedaoo, R. K.; Tatiya, P. D.; Mahulikar, P. P.; Gite, V. V. Fabrication of dendritic 0 G PAMAM-based novel polyurea microcapsules for encapsulation of herbicide and release rate from polymer shell in different environment. *Des. Monomers Polym.* **2013**, *17*, 111−125.

(15) Hedaoo, R. K.; Gite, V. V. Renewable resource-based polymeric microencapsulation of natural pesticide and its release study: an alternative green approach. *RSC Adv.* **2014**, *4*, 18637−18642.

(16) Jiang, W.; Zhou, G.; Duan, J.; Liu, D.; Zhang, Q.; Tian, F. Synthesis and Characterization of a Multifunctional Sustained-Release Organic-Inorganic Hybrid Microcapsule with Self-Healing and Flame-Retardancy Properties. *ACS Appl. Mater. Interfaces* **2021**, *13*, 15668−15679.

(17) Kumar, S.; Bhanjana, G.; Sharma, A.; Sidhu, M. C.; Dilbaghi, N. Synthesis, characterization and on field evaluation of pesticide loaded

sodium alginate nanoparticles. *Carbohydr. Polym.* **2014**, *101*, 1061−1067.
(18) Yang, J.; Zhou, Z.; Liang, Y.; Tang, J.; Gao, Y.; Niu, J.; Dong, H.; Tang, R.; Tang, G.; Cao, Y. Sustainable Preparation of Microcapsules with Desirable Stability and Bioactivity Using Phosphonium Ionic Liquid as a Functional Additive. *ACS Sustain. Chem. Eng.* **2020**, *8*, 13440−13448.
(19) Butstraen, C.; Salaün, F. Preparation of microcapsules by complex coacervation of gum Arabic and chitosan. *Carbohydr. Polym.* **2014**, *99*, 608−616.
(20) Dai, R. Y.; You, S. Y.; Lu, L. M.; Liu, Q.; Li, Z. X.; Wei, L.; Huang, X. G.; Yang, Z. Y. High blades spreadability of chlorpyrifos microcapsules prepared with polysiloxane sodium carboxylate/sodium carboxymethylcellulose/gelatin via complex coacervation. *Colloids Surf., A* **2017**, *530*, 13−19.
(21) Shi, T.; Hu, P.; Wang, J. Preparation of Polyurea Microcapsules Containing Phase Change Materials Using Microfluidics. *ChemistrySelect* **2020**, *5*, 2342−2347.
(22) Cao, H.; Zhang, D.-x.; Liu, S.; Luo, J.; Jing, T.; Pan, S.; Liu, F.; Li, B.; Mu, W. Achieving Win-Win Ecotoxicological Safety and Fungicidal Activity of Pyraclostrobin-Loaded Polyurea Microcapsules by Selecting Proper Polyamines. *J. Agric. Food Chem.* **2021**, *69*, 2099−2107.
(23) Zhan, S.; Chen, S.; Chen, L.; Hou, W. Preparation and characterization of polyurea microencapsulated phase change material by interfacial polycondensation method. *Powder Technol.* **2016**, *292*, 217−222.
(24) Zhong, F.; Yang, C.; Wu, Q.; Wang, S.; Cheng, L.; Dwivedi, P.; Zhu, Z.; Si, T.; Xu, R. X. Preparation of pesticide-loaded microcapsules by liquid-driven coaxial flow focusing for controlled release. *Int. J. Polym. Mater. Polym. Biomater.* **2019**, *69*, 840−847.
(25) Ravanfar, R.; Comunian, T. A.; Dando, R.; Abbaspourrad, A. Optimization of microcapsules shell structure to preserve labile compounds: A comparison between microfluidics and conventional homogenization method. *Food Chem.* **2018**, *241*, 460−467.
(26) Paquet, C.; Jakubek, Z. J.; Simard, B. Superparamagnetic microspheres with controlled macroporosity generated in microfluidic devices. *ACS Appl. Mater. Interfaces* **2012**, *4*, 4934−4941.
(27) Lin, P.; Chen, H.; Li, A.; Zhuang, H.; Chen, Z.; Xie, Y.; Zhou, H.; Mo, S.; Chen, Y.; Lu, X.; Cheng, Z. Bioinspired Multiple Stimuli-Responsive Optical Microcapsules Enabled by Microfluidics. *ACS Appl. Mater. Interfaces* **2020**, *12*, 46788−46796.
(28) Michelon, M.; Leopércio, B. C.; Carvalho, M. S. Microfluidic production of aqueous suspensions of gellan-based microcapsules containing hydrophobic compounds. *Chem. Eng. Sci.* **2020**, *211*, 115314−115325.
(29) Liu, J.; Lan, Y.; Yu, Z.; Tan, C. S. Y.; Parker, R. M.; Abell, C.; Scherman, O. A. Cucurbit[n]uril-Based Microcapsules Self-Assembled within Microfluidic Droplets: A Versatile Approach for Supramolecular Architectures and Materials. *Acc. Chem. Res.* **2017**, *50*, 208−217.
(30) Zhang, L.; Liu, Z.; Liu, L.-Y.; Ju, X.-J.; Wang, W.; Xie, R.; Chu, L.-Y. Novel Smart Microreactors Equipped with Responsive Catalytic Nanoparticles on Microchannels. *ACS Appl. Mater. Interfaces* **2017**, *9*, 33137−33148.
(31) Lin, P.; Wei, Z.; Yan, Q.; Xie, J.; Fan, Y.; Wu, M.; Chen, Y.; Cheng, Z. Capillary-Based Microfluidic Fabrication of Liquid Metal Microspheres toward Functional Microelectrodes and Photothermal Medium. *ACS Appl. Mater. Interfaces* **2019**, *11*, 25295−25305.
(32) Huang, L.; Wu, K.; He, X.; Yang, Z.; Ji, H. One-Step microfluidic synthesis of spherical and bullet-like alginate microcapsules with a core-shell structure. *Colloids Surf., A* **2021**, *608*, 125612−125621.
(33) Xu, B.; Guo, J.; Fu, Y.; Chen, X.; Guo, J. A review on microfluidics in the detection of food pesticide residues. *Electrophoresis* **2020**, *41*, 821−832.
(34) Xie, J.; Pang, H.; Sun, R.; Wang, T.; Meng, X.; Zhou, Z. Development of Rapid and High-Precision Colorimetric Device for Organophosphorus Pesticide Detection Based on Microfluidic Mixer Chip. *Micromachines* **2021**, *12*, 290−303.
(35) Tahirbegi, I. B.; Ehgartner, J.; Sulzer, P.; Zieger, S.; Kasjanow, A.; Paradiso, M.; Strobl, M.; Bouwes, D.; Mayr, T. Fast pesticide detection inside microfluidic device with integrated optical pH, oxygen sensors and algal fluorescence. *Biosens. Bioelectron.* **2017**, *88*, 188−195.
(36) Rai, A.; Sibi, M. G.; Farooqui, S. A.; Anand, M.; Bhaumik, A.; Sinha, A. K. Mesoporous γ-Alumina with Isolated Silica Sites for Direct Liquid Hydrocarbon Production during Fischer-Tropsch Reactions in Microchannel Reactor. *ACS Sustain. Chem. Eng.* **2017**, *5*, 7576−7586.
(37) Zait, Y.; Segev, D.; Schweitzer, A.; Goldwasser, Y.; Rubin, B.; Mishael, Y. G. Development and employment of slow-release pendimethalin formulations for the reduction of root penetration into subsurface drippers. *J. Agric. Food Chem.* **2015**, *63*, 1682−1688.
(38) Liang, Y.; Guo, M.; Fan, C.; Dong, H.; Ding, G.; Zhang, W.; Tang, G.; Yang, J.; Kong, D.; Cao, Y. Development of Novel Urease-Responsive Pendimethalin Microcapsules Using Silica-IPTS-PEI As Controlled Release Carrier Materials. *ACS Sustain. Chem. Eng.* **2017**, *5*, 4802−4810.
(39) Zhang, D.-x.; Zhang, X.-p.; Luo, J.; Li, B.-x.; Wei, Y.; Liu, F. Causation Analysis and Improvement Strategy for Reduced Pendimethalin Herbicidal Activity in the Field after Encapsulation in Polyurea. *ACS Omega* **2018**, *3*, 706−716.
(40) Huang, B.; Li, J.; Fang, W.; Liu, P.; Guo, M.; Yan, D.; Wang, Q.; Cao, A. Effect of soil fumigation on degradation of pendimethalin and oxyfluorfen in laboratory and ginger field studies. *J. Agric. Food Chem.* **2016**, *64*, 8710−8721.
(41) Zhang, X.-p.; Luo, J.; Zhang, D.-x.; Jing, T.-f.; Li, B.-x.; Liu, F. Porous microcapsules with tunable pore sizes provide easily controllable release and bioactivity. *J. Colloid Interface Sci.* **2018**, *517*, 86−92.
(42) Zhang, X.-p.; Luo, J.; Jing, T.-f.; Zhang, D.-x.; Li, B.-x.; Liu, F. Porous epoxy phenolic novolac resin polymer microcapsules: Tunable release and bioactivity controlled by epoxy value. *Colloids Surf., B* **2018**, *165*, 165−171.
(43) Ren, L.; Huang, B.; Fang, W.; Zhang, D.; Cheng, H.; Song, Z.; Yan, D.; Li, Y.; Wang, Q.; Zhou, Z.; Cao, A. Multi-Encapsulation Combination of O/W/O Emulsions with Polyurea Microcapsules for Controlled Release and Safe Application of Dimethyl Disulfide. *ACS Appl. Mater. Interfaces* **2021**, *13*, 1333−1344.
(44) Polenz, I.; Datta, S. S.; Weitz, D. A. Controlling the morphology of polyurea microcapsules using microfluidics. *Langmuir* **2014**, *30*, 13405−13410.
(45) Jiang, X.; Bashir, M. S.; Zhang, F.; Kong, X. Z. Formation and shape transition of porous polyurea of exotic forms through interfacial polymerization of toluene diisocyanate in aqueous solution of ethylenediamine and their characterization. *Eur. Polym. J.* **2018**, *109*, 93−100.
(46) Zhang, F.; Jiang, X.; Zhu, X.; Chen, Z.; Kong, X. Z. Preparation of uniform and porous polyurea microspheres of large size through interfacial polymerization of toluene diisocyanate in water solution of ethylene diamine. *Chem. Eng. J.* **2016**, *303*, 48−55.
(47) Wu, K.-J.; Nappo, V.; Kuhn, S. Hydrodynamic Study of Single- and Two-Phase Flow in an Advanced-Flow Reactor. *Ind. Eng. Chem. Res.* **2015**, *54*, 7554−7564.
(48) Zhang, F.; Cerato-Noyerie, C.; Woehl, P.; Lavric, E. D. Intensified Liquid/Liquid Mass Transfer in Corning Advanced-Flow Reactors. *Chem. Eng. Trans.* **2011**, *24*, 1369−1378.
(49) Nieves-Remacha, M. J.; Kulkarni, A. A.; Jensen, K. F. Gas-Liquid Flow and Mass Transfer in an Advanced-Flow Reactor. *Ind. Eng. Chem. Res.* **2013**, *52*, 8996−9010.
(50) Nieves-Remacha, M. J.; Kulkarni, A. A.; Jensen, K. F. Hydrodynamics of Liquid-Liquid Dispersion in an Advanced-Flow Reactor. *Ind. Eng. Chem. Res.* **2012**, *51*, 16251−16262.
(51) Polenz, I.; Weitz, D. A.; Baret, J.-C. Polyurea microcapsules in microfluidics: surfactant control of soft membranes. *Langmuir* **2015**, *31*, 1127−1134.

https://doi.org/10.1021/acsomega.1c05903
ACS Omega 2021, 6, 34160−34172

(52) Wang, H.; Wang, J. P.; Wang, X.; Li, W.; Zhang, X. Preparation and Properties of Microencapsulated Phase Change Materials Containing Two-Phase Core Materials. *Ind. Eng. Chem. Res.* **2013**, *52*, 14706−14712.
(53) Kong, F.; Zhang, X.; Hai, M. Microfluidics Fabrication of Monodisperse Biocompatible Phospholipid Vesicles for Encapsulation and Delivery of Hydrophilic Drug or Active Compound. *Langmuir* **2014**, *30*, 3905−3912.

https://doi.org/10.1021/acsomega.1c05903
ACS Omega 2021, 6, 34160−34172